Role of turgor pressure in endocytosis in fission yeast

Roshni Basu*, Emilia Laura Munteanu, and Fred Chang
Department of Microbiology and Immunology, Columbia University College of Physicians and Surgeons, New York, NY 10032

ABSTRACT **Yeast and other walled cells possess high internal turgor pressure that allows them to grow and survive in the environment. This turgor pressure, however, may oppose the invagination of the plasma membrane needed for endocytosis. Here we study the effects of turgor pressure on endocytosis in the fission yeast *Schizosaccharomyces pombe* by time-lapse imaging of individual endocytic sites. Decreasing effective turgor pressure by addition of sorbitol to the media significantly accelerates early steps in the endocytic process before actin assembly and membrane ingression but does not affect the velocity or depth of ingression of the endocytic pit in wild-type cells. Sorbitol also rescues endocytic ingression defects of certain endocytic mutants and of cells treated with a low dose of the actin inhibitor latrunculin A. Endocytosis proceeds after removal of the cell wall, suggesting that the cell wall does not contribute mechanically to this process. These studies suggest that endocytosis is governed by a mechanical balance between local actin-dependent inward forces and opposing forces from high internal turgor pressure on the plasma membrane.**

Monitoring Editor
David G. Drubin
University of California, Berkeley

Received: Oct 24, 2013
Revised: Dec 27, 2013
Accepted: Dec 30, 2013

INTRODUCTION

Endocytosis involves the formation of a local invagination of the plasma membrane that resolves into an endocytic vesicle. In both fission and budding yeast cells, proteins have been found to assemble and disassemble at the endocytic site in a highly choreographed, dynamic sequence of events that take ~100 s (Merrifield *et al.*, 2004; Sirotkin *et al.*, 2005, 2010; Kaksonen *et al.*, 2006; Galletta and Cooper, 2009; Berro *et al.*, 2010; Basu and Chang, 2011; Boettner *et al.*, 2012; Weinberg and Drubin, 2012). Initially, early proteins such as clathrin and early coat proteins arrive at the membrane, followed by cargo molecules and then intermediate and the late coat proteins. About 30 s after the arrival of the adaptor proteins, a local burst of Arp2/3 complex–dependent actin polymerization occurs at the site. This is followed by the rapid ingression of the membrane to form a narrow endocytic pit. Membrane scission at the neck of the pit then liberates the endocytic vesicle. Proteins that contribute to membrane curvature, such as BAR-domain proteins and dynamin, as well as local changes in phosphoinositide composition, contribute to dynamic reorganization of the plasma membrane. In budding and fission yeast, actin is critical for multiple steps in this process, including invagination, membrane scission, and recruitment of other endocytic proteins (Mulholland *et al.*, 1994; Ayscough, 2000; Engqvist-Goldstein and Drubin, 2003; Merrifield *et al.*, 2004; Kaksonen *et al.*, 2005, 2006; Newpher *et al.*, 2005; Girao *et al.*, 2008; Galletta and Cooper, 2009; Robertson *et al.*, 2009; Berro *et al.*, 2010; Sirotkin *et al.*, 2010; Basu and Chang, 2011; Weinberg and Drubin, 2012). A similar sequence of events occurs in clathrin-mediated endocytosis in animal cells (Taylor *et al.*, 2011), although the requirement for actin is less clear. Actin is generally believed to be dispensable for invagination but is needed in subsequent steps, such as scission and movement of the endocytic vesicle in the cytoplasm (Merrifield *et al.*, 2002, 2005). However, it has been shown to be important for membrane invagination in certain circumstances, such as at the apical surface of epithelial cells (Boulant *et al.*, 2011) and in the absence of dynamin (Ferguson *et al.*, 2009).

One key difference between animal cells and walled cells such as those in yeast, plants, and bacteria is the presence of high turgor

This article was published online ahead of print in MBoC in Press (http://www.molbiolcell.org/cgi/doi/10.1091/mbc.E13-10-0618) on January 8, 2014.

*Present address: Department of Immunology, Memorial Sloan-Kettering Cancer Center, New York, NY 10065.

Address correspondence to: Fred Chang (fc99@columbia.edu).

Abbreviation used: LatA, latrunculin A.

pressure in the walled cells. Measurements of the mechanical properties have shown that fission yeast cells have high turgor pressures, on the order of 1–1.5 MPa (1 MPa = 10 atm or 145 psi, similar to pressure in a racing bike tire; Minc *et al.*, 2009; our unpublished observations). Similar turgor pressures have been estimated in budding yeast (Schaber *et al.*, 2010). To support this internal pressure, the fission yeast cell is encased in an elastic cell wall with a Young's modulus of ~20 N/m (elasticity similar to a hard tire rubber; Minc *et al.*, 2009). These measurements predict that indenting the plasma membrane into the cell interior may require substantial inward forces against this large outward force from turgor pressure. Recent work shows that turgor pressure may oppose the ingression of the plasma membrane during cleavage for cytokinesis in fission yeast; addition of sorbitol, which reduces effective turgor pressure, causes ingression of the septum to proceed faster (Proctor *et al.*, 2012). Aghamohammadzadeh and Ayscough (2009) showed initial results suggesting that turgor pressure is also a factor in endocytosis in budding yeast.

Here we pursue a quantitative analysis of the effects of turgor pressure on endocytosis in fission yeast. Our results show that lowering effective turgor pressure can make an early step in endocytosis proceed up to 40% faster and ameliorate endocytic defects in cells with reduced actin dynamics. Thus these findings demonstrate that turgor pressure is a significant factor in endocytosis. On the assumption that elements of the patch need to work against 1 MPa pressure, these results provide initial estimates that hundreds of piconewtons of force is needed for membrane invagination in yeast endocytosis.

RESULTS

Reducing turgor pressure accelerates early endocytic events

To monitor endocytic events in living cells, we imaged two representative endocytic proteins, sla1p and coronin crn1p (Supplemental Movie S1; Basu and Chang, 2011). Sla1p, an adaptor protein, arrives early in the endocytic process, before the burst of actin polymerization, whereas crn1p, whose localization is actin dependent, arrives concurrent with actin polymerization. In time-lapse imaging of cells coexpressing sla1-GFP and crn1-Tomato, we observed that sla1p patches appeared on the cortex at the site of endocytosis and were stationary for an average of 19.6 ± 5.1 s (n = 20 patches) before moving inward into the cell interior. At 17.4 ± 5.4 s after sla1p arrival, crn1p appeared at the site for 2.2 ± 2.5 s before moving inward with sla1p (Figure 1). This inward movement of the markers likely represents the movement of the base of the endocytic pit into the cell interior (Idrissi *et al.*, 2008, 2012). We term this detectable inward movement "ingression." Subsequently, sla1p and crn1p disassociated from the patch structure after 14.5 ± 4.8 and 19.8 ± 8.2 s, respectively (Supplemental Figure S1; Pelham and Chang, 2001; Sirotkin *et al.*, 2010). We also imaged the actin-binding proteins app1–green fluorescent protein (GFP; Abp1 orthologue) and fim1-GFP (fimbrin) as markers for actin filaments at the endocytic site (Supplemental Figure S1; Morrell *et al.*, 1999; Pelham and Chang, 2001). Time-lapse imaging of these various markers thus provides a way to probe the dynamic progression of events at the endocytic site.

We hypothesized that high internal turgor pressure opposes the inward movement of the plasma membrane during endocytosis. To test this, we examined the effects of reducing turgor pressure on endocytosis by adding different concentrations of sorbitol to the media. High concentrations of sorbitol (>0.4 M, which is equivalent to 1 MPa) cause cells to shrink, and so we used much lower sorbitol concentrations. Cells respond to sorbitol through osmotic shock pathways by inducing the synthesis of intracellular glycerol (Aiba *et al.*, 1995; Degols *et al.*, 1996; Hohmann, 2002). This adaptive process, however, takes 15–60 min. We therefore used two ways to minimize these compensatory effects.

First, we added sorbitol to wild-type cells and assayed effects within 1–5 min, before cells fully adapt. This treatment did not inhibit endocytosis, as all patches internalized (Figure 1C and Supplemental Movie S2). Sorbitol caused a significant dose-dependent shortening of the time period in which sla1-GFP resides at the cortical site before crn1-Tomato arrival (Figure 1D, green, and Supplemental Figure S1A). At 0.2 M sorbitol, this period was shortened by 43% (11.1 ± 2.7 s, n = 20 patches). The period of crn1p on the cell surface was also slightly shortened (Figure 1D, yellow), but these differences were not statistically significant. Similar findings were seen with patches marked with app1-GFP and fim1-GFP (Supplemental Figure S1). Sorbitol caused significant decrease in the time spent by app1p and fim1p (shortened by 34 and 30% at 0.2 M sorbitol, respectively; Supplemental Figure S1). Sorbitol did not affect significantly the behavior of these markers after patch internalization (Supplemental Figure S1). Thus these data suggest that reduction in relative turgor pressure may cause acceleration of the early period of endocytosis.

Second, we examined the effect of sorbitol in a mutant lacking gpd1p (glycerol-3-phosphate dehydrogenase), the enzyme principally responsible for increasing glycerol production upon osmotic stress. The *gpd1*-null mutant cells have strong defects in adapting to changes in turgor pressure, and thus effects of sorbitol can be assayed in a more direct manner (Aiba *et al.*, 1995; Degols *et al.*, 1996; Hohmann, 2002; Minc *et al.*, 2009). A low dose (0.05 M) of sorbitol to *gpd1Δ* cells led to 21% decrease in the period of sla1p at the cortex as compared with the period in *gpd1Δ* cells without sorbitol (5.2 vs. to 6.7 s; n = 20 patches each; Figure 1D). Note that in *gpd1Δ* cells even without sorbitol addition, the sla1p period was shorter compared with wild-type cells; the reasons are not clear, as these cells may not have significantly reduced turgor pressure (E. Atilgan and F. Chang, unpublished observations).

We tested whether the increase in patch dynamics by sorbitol may be due to changes in the concentration of patch proteins such as actin. Fluorescence intensity measurements of the actin markers fim1p and app1p were not significantly affected by 0.025 M sorbitol treatment (Supplemental Figure S1).

These data show that reducing turgor pressure can accelerate early stages of endocytosis before patch internalization in a dramatic manner, by up to 40%.

Effect of sorbitol on the rate of membrane ingression

Next we investigated whether sorbitol has an effect on the rate of patch movement during internalization. We tracked the movement of individual patches over time through subpixel-resolution tracking of sla1-GFP patches. Immuno–electron microscopy showed that budding yeast Sla1 (orthologue of *Schizosaccharomyces pombe* sla1p) is present at the base of the endocytic pit in budding yeast (Idrissi *et al.*, 2008, 2012). If we assume that this cluster of *S. pombe* sla1-GFP molecules marks the base of the pit as a point source, we could track the base of the pit with subpixel resolution (see *Materials and Methods*). Using this approach, we found that sla1-GFP patches were initially stationary on the cell cortex and then moved ~300 nm into the cell interior in a biphasic pattern: a first phase of average velocity of 0.033 μm/s, and second phase with a faster final rate of 0.067 μm/s (Figure 1, E and F; n = 20 patches). Patches subsequently paused and then often changed directions; this may correspond to vesicle scission (Figure 1E). Our ingression rate measurements are in

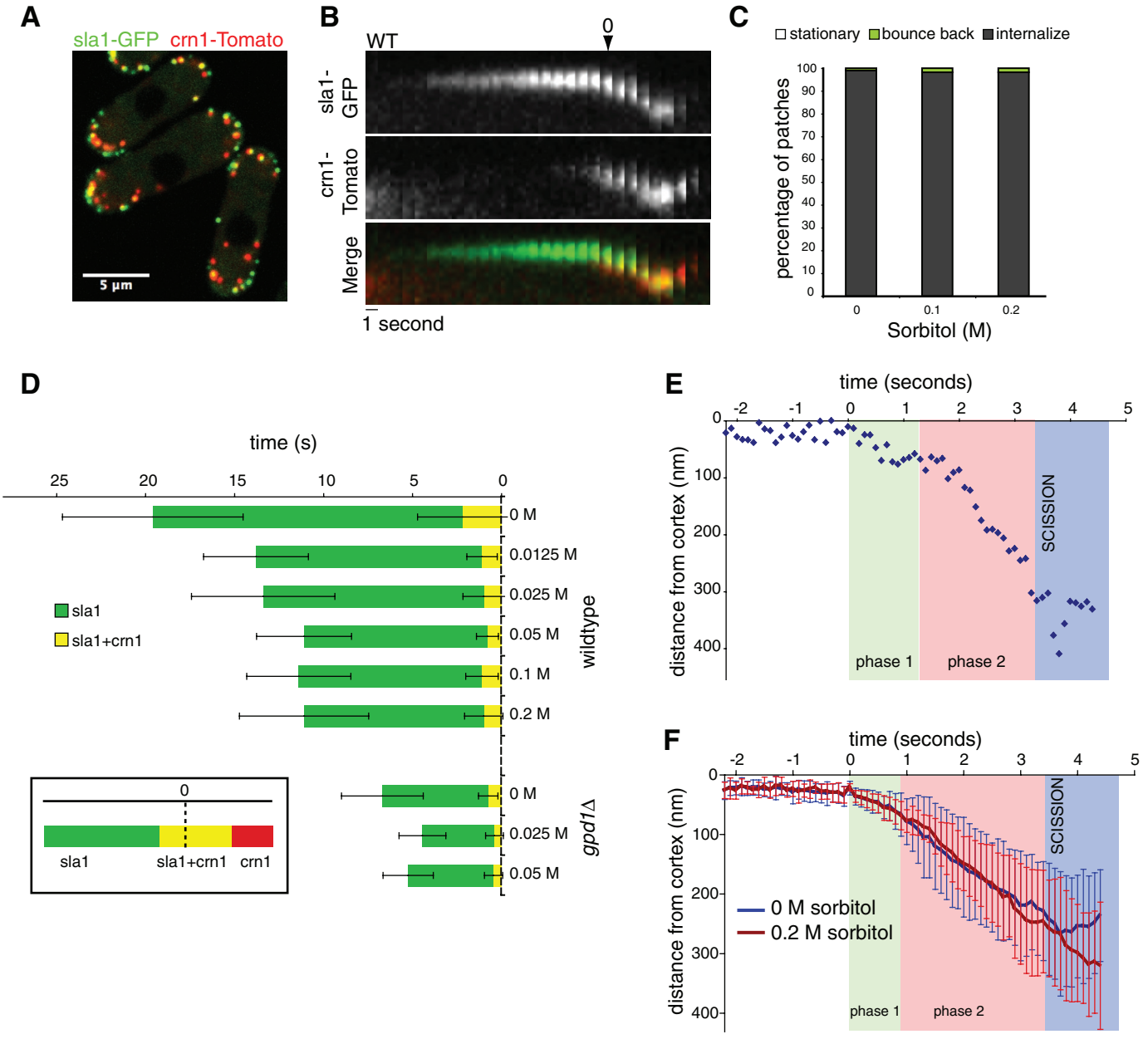

FIGURE 1: Addition of sorbitol to the media accelerates initial events of endocytosis. (A) Three fission yeast cells expressing endocytic patch markers sla1-GFP (adaptor protein, green) and crn1-Tomato (coronin; red; FC2589). Medial focal plane confocal image. (B) Time-lapse images of a single endocytic patch marked sla1-GFP and crn1-Tomato in wild-type cell. The onset of inward movement is designated as time 0. Images are shown at 1-s intervals. (C) Behavior of patches in wild-type cells at indicated sorbitol concentrations. For each condition $n = 56$ patches. (D) Average residence time of sla1-GFP and crn1-Tomato at the cortex before ingression (at $t = 0$) in wild-type (FC2589) and *gpd1Δ* (FC2592) cells in the indicated sorbitol concentrations. These are temporal maps of patch behavior, where green is the period during which the patch contains sla1-GFP without crn1-Tomato, and yellow denotes when both proteins are present. For each condition $n = 20$ patches. (E) Track of a representative sla1-GFP patch in a wild-type cell. Images were acquired every 100 ms in a single confocal plane, and positions of the patches were determined with subpixel resolution (*Materials and Methods*). Time 0 is onset of detectable movement into the cell. Note that there are at least two phases of inward movement with different rates, followed by a transition to more random movement, which may represent time of scission. (F) Average distance traveled inward from the plasma membrane by sla1-GFP patches in wild-type cells in 0 (blue) and 0.2 M (red) sorbitol. $n = 20$ and 19 patches, respectively. Error bars, SD.

the range of previous estimates in fission yeast of 0.06–0.1 µm/s (Sirotkin *et al.*, 2010). Our depth measurements in live cells are larger than the dimensions of the budding yeast endocytic pit measured by electron microscopy (Idrissi *et al.*, 2008; Kishimoto *et al.*, 2011; Kukulski *et al.*, 2012). Of interest, addition of 0.2 M sorbitol had little effect on inward rate or depth of movement in wild-type *S. pombe* cells ($n = 19$ cells). Sorbitol also had little effect on rates and depths of ingression in *gpd1Δ* cells (Supplemental Figure S2). Thus, although sorbitol affects the initial stages of endocytosis, it does not affect the actual ingression process.

Reducing turgor pressure partially suppresses the requirement for actin polymerization during endocytosis

We next asked whether reducing effective turgor pressure rescues cells that are defective in endocytosis. First, we tested whether sorbitol suppresses the endocytic defects seen in cells treated with 2 μM latrunculin A (LatA), an inhibitor of actin polymerization. At this low dose of latrunculin A, actin filaments are still present at patches, but the patches do not move inward detectably (98% of patches; $n = 53$ patches; Figure 2; Basu and Chang, 2011). These patches may not be able to ingress because they lack a burst of actin polymerization that usually precedes ingression (Basu and Chang, 2011).

The addition of sorbitol rescued the ingression defect in these LatA-treated cells. We examined the effects of adding sorbitol within 1–5 min. At 0.2 M sorbitol, ~90% of patches moved inward ($n = 56$ patches). However, sla1-GFP patches traveled inward for only about one- sixth of the normal distance (~50 nm), and the rate of movement was ~10-fold slower than the initial movement in wild-type cells (0.003 μm/s; $n = 15$ patches; Figure 1F). In addition, instead of fully internalizing, most patches then appeared to spring back to the cortex (Figure 2). This kind of "bounce-back" behavior is similar to that of mutants defective in scission, such as F-BAR protein mutants (e.g., *bzz1*) and mutants in actin regulation (e.g. *wsp1*; Arasada and Pollard, 2011; Basu and Chang, 2011; Kishimoto *et al.*, 2011). Thus sorbitol addition may allow endocytic pits with a compromised actin cytoskeleton to move partially inward but not to fully undergo scission.

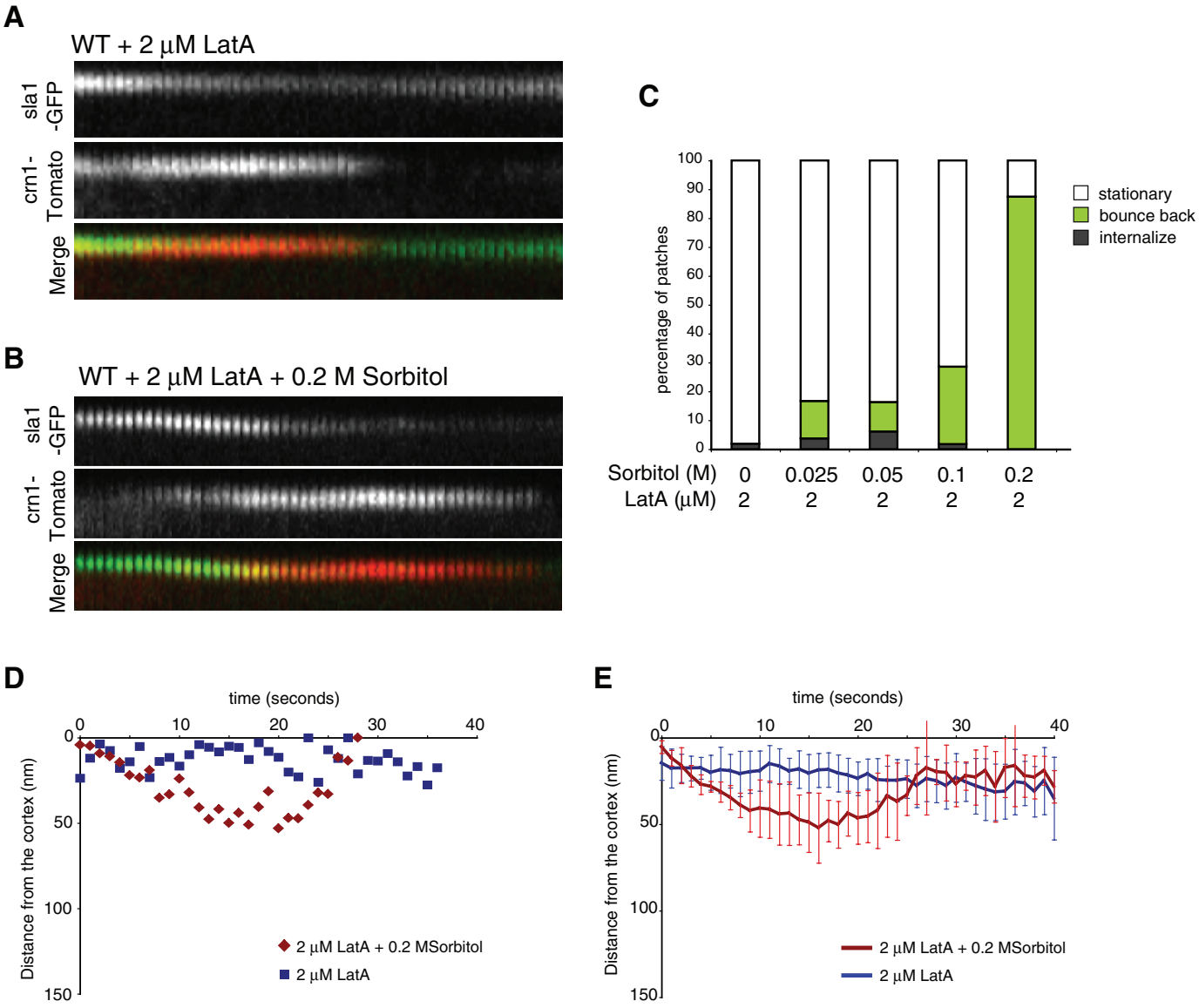

FIGURE 2: Sorbitol rescues endocytic ingression defects of cells treated with a low dose of latrunculin A. (A) Time-lapse images of a single patch containing sla1-GFP and crn1-Tomato (FC2589) after treatment with 2 μM LatA. (B) Time-lapse images of a single patch after treatment with 2 μM LatA and 0.2 M sorbitol. Images acquired at 1-s intervals. (C) Behavior of patches in wild-type cells treated with 2 μM LatA and at indicated sorbitol concentrations. The behavior of each patch was categorized as those that remain stationary at the cortex (as in A), those that move inward but bounce back (as in B), and those that internalize successfully. For each condition $n = 56$ patches. (D) Tracks of individual sla1-GFP patches in wild-type cells in 2 μM LatA and 0 (blue) or 0.2 M (red) sorbitol. (E) Average distances of patches from the cortex, as described in D. $n = 18$ and 15 patches, respectively. Error bars, SD.

Sorbitol, however, could not compensate for total loss of actin. In cells treated with a high dose of LatA (200 μM for 10 min), which causes depolymerization of all detectable actin filaments (Chang, 1999; Pelham and Chang, 2001), sla1-GFP–marked patches appeared and persisted on the cell surface for the entire length of the movie (50 s) without detectable movement (n = 100 patches; Supplemental Figure S3). Addition of 0.1–0.4 M sorbitol did not suppress this defect. Thus a minimal amount of F-actin is required for patch ingression in sorbitol.

Reducing turgor pressure rescues endocytic mutants

We tested whether reducing turgor pressure could rescue defects in representative endocytic mutants. Wsp1p (WASp) and myo1p (myosin I) are activators of Arp2/3 complex–mediated actin assembly and are necessary for efficient endocytosis (Sirotkin *et al.*, 2005; Basu and Chang, 2011). Myosin I is the primary myosin present at endocytic sites and thus may contribute to actin-based force production for endocytosis. In *wsp1*- and *myo1*-null mutants, patches form with some F-actin but fail in ingression (Sirotkin *et al.*, 2005; Arasada and Pollard, 2011; Basu and Chang, 2011). We found that 85% of *wsp1Δ* patches remained stationary at the cell cortex. Addition of 0.1 M sorbitol led to ingression of 90% of patches and to full internalization of 55% of patches (Figure 3A). Similarly, 80% of *myo1Δ* patches remained stationary at the cell cortex in the absence of sorbitol, and 82% of patches ingressed in 0.1 M sorbitol, with 70% of patches exhibiting full internalization (Figure 3B). For reasons that are unclear, addition of a higher dose to 0.2 M sorbitol rescued more poorly than 0.1 M in both *wsp1Δ* and *myo1Δ* mutants.

We also examined an *arp2* mutant (component of the Arp2/3 complex). In this partial loss-of-function mutant *arp2-1* (Morrell *et al.*, 1999) all patches ingressed but only after long delays at the cell surface (sla1p resident time, 31.3 ± 7.6 s; n = 20 patches; Figure 3C). Addition of sorbitol significantly rescued this delay (18.7 ± 5.4 s at 0.025 M sorbitol; 41% less than at 0 M sorbitol).

In addition to actin assembly, bundling of actin filaments is also likely to be critical for force production. The actin-bundling protein fimbrin is a patch protein required for efficient endocytosis (Wu *et al.*, 2001; Gheorghe *et al.*, 2008; Skau and Kovar, 2010). We found that in *fim1* (fimbrin) mutant cells, only 10% of patches fully internalized, whereas in 0.2 M sorbitol, 87% did (n = 40 and 62 patches respectively; Figure 3D).

Sorbitol, however, did not rescue all endocytic mutants. In the *end4* mutant (Sla2, Hip1-related adaptor protein), patches form abnormal actin comet tail structures (Wu *et al.*, 2001; Sirotkin *et al.*, 2010). Fifty-four percent of patches in this mutant did not ingress. Sorbitol did not rescue this defect (46% in 0.05 M sorbitol; $n > 70$ patches) and inhibited ingression entirely at 0.1 M (Figure 3E). In these mutant cells, the actin cytoskeleton is believed to be uncoupled from the plasma membrane (Skruzny *et al.*, 2012) and may therefore have defects that cannot be rescued by reduction in turgor pressure. Inhibitory effects of higher doses of sorbitol (e.g., 0.2 M), which were seen in *wsp1Δ*, *myo1Δ*, *end4Δ*, and *gpd1Δ* mutants (Figures 1 and 3), may be caused by adverse effects of sorbitol on global cell physiology in addition to local effects at endocytic pits. Nevertheless, the impressive rescue of WASp, myosin I, and fimbrin mutants, as well as LatA-treated cells, supports the idea that a primary function of actin and these factors is to provide mechanical forces opposing turgor pressure.

The cell wall is not required for endocytosis

Endocytosis and the cell wall share a close relationship in fungal and plant cells. For instance, regions of endocytosis correlate with regions of active cell wall growth and remodeling. Cell wall synthesis has been proposed to facilitate membrane invaginations in bacteria (Meyer *et al.*, 2010). In fungal cytokinesis, cell wall assembly at the septum is believed to provide most of the force for ingression of plasma membrane against turgor pressure (Proctor *et al.*, 2012). We tested whether the cell wall similarly contributes force for endocytic ingression or somehow shields or stabilizes the plasma membrane from turgor pressure.

To test the role of the cell wall, we removed the cell wall by enzymatic digestion to generate protoplasts. These were maintained in media with 0.2–0.5 M sorbitol for osmotic support to prevent cell lysis. Because of the long incubation periods in sorbitol, these cells adapt their internal turgor pressures to the extracellular sorbitol concentration. Protoplasts formed endocytic patches, although they were no longer in a polarized distribution (Figure 4A). Time-lapse imaging revealed that these patches were still dynamic. Measurements showed no significant change in cortical residence times of patches: sla1-GFP and crn1-Tomato remained at the cortex for 13.0 ± 3.8 and 2.7 ± 0.7 s, respectively, in the presence of a cell wall and for 11.7 ± 2.9 and 2.9 ± 1.6 s, respectively, in protoplasts (n = 10; Figure 4B). Depth of ingression was similar to that in intact cells, although rate of membrane ingression in the protoplasts was about twofold slower (Figure 4C). These results are consistent with a previous finding in which endocytic uptake of pheromone continues in budding yeast spheroplasts (deHart *et al.*, 2003). Thus the cell wall is not required for efficient endocytosis in these cells.

DISCUSSION

These studies indicate that turgor pressure is a factor in the mechanics of endocytosis in fission yeast. We show that reducing the effective turgor pressure accelerates progression of early endocytic events in wild-type cells and compensates for defects in endocytic mutants affected in actin assembly, cross-linking, and myosin I. Decreasing turgor pressure has effects on multiple aspects of endocytosis: it dramatically increases the rate of progression of initial events leading up to actin polymerization and ingression and also compensates for subsequent actin-dependent defects in ingression and scission. We postulate that turgor pressure introduces outward tension on the plasma membrane; addition of sorbitol may allow the membrane to be more amenable to inward deformations needed for endocytosis to progress.

Precisely how sorbitol affects membrane deformations is unclear. The mechanism and timing of initial indentation of the plasma membrane in wild-type cells are not well established. A cryo–electron tomography study in budding yeast showed that the plasma membrane is flat before the arrival of F-actin and that indentation of the plasma membrane is actin dependent (Kukulski *et al.*, 2012). In contrast, immuno–electron microscopy studies in budding yeast using chemical fixation show that indentation of the membrane occurs early and is independent of actin and clathrin (Idrissi *et al.*, 2008, 2012). It remains to be seen when membrane deformations occur in fission yeast and how sorbitol alters membrane topology. In our light microscopy–based assays, small initial deformations would not be detectable.

These studies begin to provide quantitative estimates for force production needed for membrane ingression for endocytosis. If we assume a turgor pressure of 1 MPa (Minc *et al.*, 2009) and the tip of the invagination to be a hemispherical structure, a simple calculation (force = pressure × surface area) leads to a plot of force required for invaginations of different sizes (Supplemental Figure S4). It is not clear, however, what size of the pit is relevant. The size of the invagination varies as the pit evolves over time: initial indentations in budding yeast have a radius of >30 nm, whereas a more mature

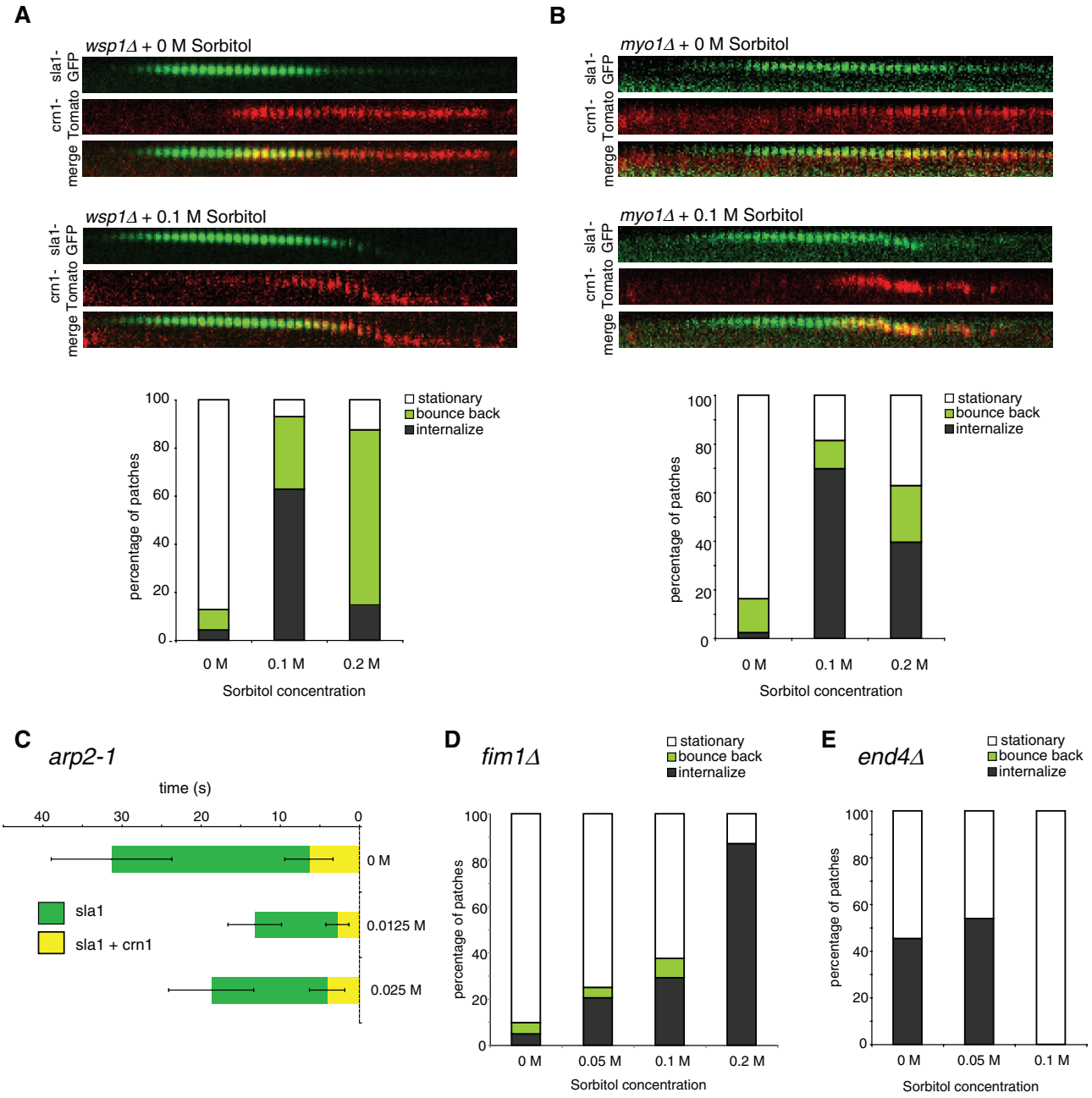

FIGURE 3: Sorbitol rescues a subset of endocytic mutants. (A) Top, time-lapse images of an individual patch containing sla1-GFP and crn1-Tomato in *wsp1Δ* (FC2587) at 0 and 0.1 M sorbitol. Images are shown at 1-s intervals. Graph shows behavior of patches. For each condition n = 47 patches. (B) Top, time-lapse images of an individual patch in *myo1Δ* (FC2659) at 0 and 0.2 M Sorbitol and graph of patch behavior. For each condition *n* = 43 patches. (C) Average residence times of sla1-GFP and crn1-Tomato at the cortex in *arp2-1* cells (FC2660) at indicated sorbitol concentrations. For each condition *n* = 20 patches. Note that all patches eventually ingress in this mutant. Bars, SD. (D) Behavior of patches in *fim1Δ* (FC2591). For each condition *n* = 48 patches. (E) Behavior of patches in *end4Δ* (FC2590). For each condition *n* = 70 patches.

pit may have a radius of ~12 nm (Kukulski *et al.*, 2012). Moreover, sizes may be different in fission versus budding yeast. If we assume that a mature endocytic pit has an outer radius of 12 nm, then the estimated force from turgor pressure in this case is ~900 pN. The forces needed for the initial shallow indentation (with >30 nm radius) may be much larger.

We considered whether actin and myosin provide sufficient force for ingression of the endocytic pit or other force-producing or compensatory mechanisms need to be invoked. Fluorescence intensity measurements suggest that each patch contains >100 of Arp2/3 complexes and capping proteins, which suggested that there are ~140 actin barbed ends in the patch (Wu and Pollard, 2005; Sirotkin *et al.*, 2010). However simulations accounting for actin polymerization rates suggest that there may be only ~8 growing actin barbed ends (Berro *et al.*, 2010). If each actin filament exerts 2 pN pushing force (Kovar and Pollard, 2004), 10 filaments would

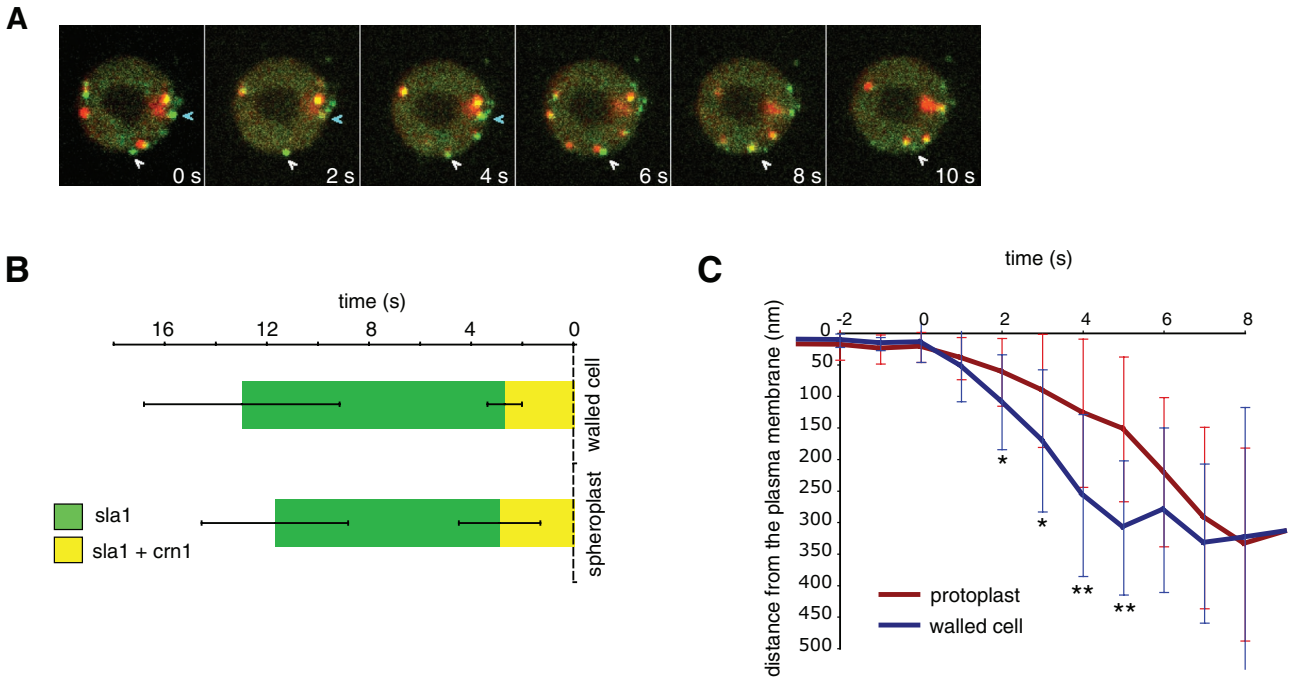

FIGURE 4: Endocytosis in the absence of the cell wall. (A) Time-lapse images of a protoplast expressing sla1-GFP (green) and crn1-Tomato (red) (FC2589). Arrowheads follow actin patches during endocytosis. (B) Average resident time of sla1-GFP and crn1-Tomato at the cortex of walled cells and protoplasts before invagination. For each condition $n = 10$ patches. (C) Average distance traveled inward by sla1-GFP patches in protoplasts and normal cells. Time 0 is beginning of inward movement. $n = 16$ and 18 patches, respectively. $^{**}p < 0.005$ and $^{*}p < 0.05$ in comparison with times at 0 M sorbitol. Error bars, SD.

provide only a very small portion (<5%) of the force needed. Myosin I, an actin motor that also binds directly to the plasma membrane, is a good candidate for producing actin-dependent forces on membranes. Three hundred myo1p (myosin I) molecules in each patch (Sirotkin *et al.*, 2010), each exerting 2 pN force (Molloy *et al.*, 1995; Veigel *et al.*, 2003), would generate maximally ~600 pN. Thus myosin I–based forces could supply the right order of magnitude of force required for invagination of a pit with a 10 nm radius but perhaps not enough for one with a 12 nm radius. More-sophisticated models for endocytosis membrane mechanics may be developed after more parameters are measured. Models incorporating the elastic nature of branched actin gels, for instance, the "elastic propulsion" model, may be considered (Mogilner and Rubinstein, 2005). Additional candidate force-producing elements at the patch may also contribute, including membrane-curving proteins such as the clathrin coat, BAR domain–containing proteins, dynamin, membrane composition, and line tension (Liu *et al.*, 2010).

These large forces needed to counter turgor pressure of 1000 nN/μm^2 are three orders of magnitude higher than actin-based forces measured in animal cells: actin comet tails formed by *Listeria* produce forces on the order of 1.5 nN/μm^2 (Giardini *et al.*, 2003) and at focal adhesions in fibroblasts and myocytes are on the order of 5 nN/μm^2 (Balaban *et al.*, 2001). In fission yeast cytokinesis, because the septum is 100 nm in width, actomyosin-based forces are not sufficient to pull the membrane for cleavage furrow ingression; instead, it is proposed that assembly of the cell wall fibers provides a large pushing force inward (Proctor *et al.*, 2012). Because of the forces for endocytic ingression are so dependent on size, mechanics may be a major constraint on the size of the endocytic pit in cells with high turgor pressure.

Our findings extend and also differ from those of Aghamohammadzadeh and Ayscough (2009), who examined similar issues in budding yeast endocytosis. These studies used much higher concentrations of sorbitol and incubation times in sorbitol of 10 min to 4 h; thus many of their findings are in cells that have adapted to high concentrations to sorbitol. Their most striking result was that sorbitol suppressed the complete loss of F-actin caused by high doses of LatA, using the internalization of the dye Lucifer yellow as an assay. We show, using movement of patch markers as an assay, that sorbitol treatment does not rescue cells treated with this high dose of LatA. Moreover, we find that even in the absence of sorbitol, *S. pombe* cells treated with high doses of LatA can still uptake Lucifer yellow into vacuoles, even though they are blocked for uptake of another membrane dye, FM4-64 (Supplemental Figure S3D, E). Thus it is likely that, at least in fission yeast, the uptake of Lucifer yellow proceeds through a distinct actin-independent mechanism.

Our findings in fission yeast are relevant to endocytosis in animal cells. Actin is critical for endocytosis at least under certain conditions. Especially because inhibitory drugs may not completely inhibit F-actin (Collins *et al.*, 2011), the role of actin in mammalian endocytosis may be in fact underappreciated. In endothelial cells, actin dynamics is required for endocytosis at the apical but not the basolateral surface (Boulant *et al.*, 2011). Mechanical stretching at the basolateral surface makes endocytosis also actin dependent, in effect, more "yeast like." At the apical surface, another myosin type I is implicated in increasing membrane tension (Nambiar *et al.*, 2009). In yeast, turgor pressure could provide a similar effect to provide tension on the membrane. Thus these actin-dependent mechanisms studied in yeast are likely to be used in animal cells.

MATERIALS AND METHODS

Yeast strains and media

The *S. pombe* strains used in this study are listed in Supplemental Table S1. Standard methods for *S. pombe* media and genetic manipulations were used (Moreno *et al.*, 1991). Tagged and deletion strains were constructed using a PCR-based approach and confirmed by analytical PCR (Bahler *et al.*, 1998). All yeast strains were grown to log phase in rich YE5S (yeast extract and amino acids) media at 25°C in exponential phase for imaging unless otherwise noted. For imaging, cells were mounted in liquid media with indicated additions on a glass slide overlaid with a glass coverslip and imaged immediately at room temperature (25–28°C).

Sorbitol and latrunculin A treatment

Cells were grown in mid exponential phase with shaking in liquid cultures in rich media YE5S at 25°C. They were treated with indicated concentrations of sorbitol (Sigma-Aldrich, St. Louis, MO) in YE5S and imaged within 1–5 min. For LatA treatments, cells were incubated in indicated concentrations of LatA for 2–5 min before image acquisition. A 20 mM stock solution of latrunculin A (Biomol International, Plymouth, PA) was prepared in dimethyl sulfoxide (Sigma-Aldrich) and was used at a range of concentrations (2–400 μM). For each set of experiments, the efficacy of the drug was confirmed by phalloidin staining of fixed samples (Chang *et al.*, 1996).

Microscopy and image analysis

Microscopy was performed using a spinning disk confocal microscope (Pelham and Chang, 2001) with a Hamamatsu electron-multiplying charge coupled device camera (Hamamatsu, Hamamatsu, Japan) with a 100×/1.4 numerical aperture oil objective and 1.5× magnifier, or a Zeiss LSM 710 laser-scanning confocal microscope. Images were acquired, processed, and analyzed with the OpenLab 5.0.2 software (Improvision, Coventry, United Kingdom), Micromanager (Edelstein *et al.*, 2010), and ImageJ software (National Institutes of Health, Bethesda, MD). In general, cortical patches were imaged in time lapse in a single medial focal plane through the cell. Although we analyzed discrete patches that appeared to be in focus, the use of the single focal plane may introduce minor variability in fluorescence intensity measurements.

Subpixel-resolution tracking of patches was performed in Matlab (MathWorks, Natick, MA). The patches marked by fluorescent proteins appear as near-resolution-sized round particles. An isotropic two-dimensional (2D) Gaussian kernel of intensities is fitted to the fluorescence image of individual patches at each time frame. The fit parameters were the position of the 2D Gaussian center, the SD of the 2D Gaussian, which is taken isotropic in all directions, the base level of intensity, and the maximum intensity at the center of the 2D Gaussian. The size of the kernel was set equal to the size of a manually cropped region containing the patch throughout the time series. The position of the patch was given by the center of the fitted 2D Gaussian. An approximate start position was manually indicated in the first frame and used as the initial input value for the fitting procedure. We measured the precision of this tracking method by analyzing stationary beads and patches (Supplemental Figure S5). We followed bead position with a precision of 6 nm for binning 1 (a field of view of 512 × 512 pixels; 33 × 33 μm) and 9 nm for binning 2 (a field of view of 256 × 256 pixels), as calculated as the SD of positions from tracking 100-nm fluorescent silica particles (0.1-μm TetraSpeck Fluorescent Microspheres; T7284; Invitrogen, Carlsbad, CA) immobilized on a glass surface (Supplemental Figure S5B). A similar precision of 6 nm (binning 1) was found in stationary sla1-GFP patches in LatA-treated living cells (Supplemental Figure S5C). In analysis of patch movements in the cell, the series of patch positions in time was then used to evaluate the distance of the patch from the cell membrane cortex. The membrane location was set manually by drawing a tangent line to the cell cortex at the patch location in the initial frame of the time series. The distance between the patch and the membrane was calculated as the perpendicular distance from the point representing the patch position to the line. The shortest distance between the tangent and the patch position was defined as 0 μm. The tracks obtained are manually aligned, where a patch is defined to begin internalizing when four consecutive patch positions show an increase in distance from the cortex.

Protoplast preparation

Cells were grown to OD_{600} of 0.5, washed with SCS buffer (20 mM citrate buffer, 1 M D-sorbitol, pH 5.8), and resuspended in 0.05 g/ml Lallzyme (Lallemand, Montreal, Canada; Flor-Parra *et al.*, 2013). Cells were incubated at 37°C with gentle shaking. After 10 min, when ~90% of the cell walls were removed, the protoplast were washed gently with SCS buffer and resuspended in YE5S with 0.25 M sorbitol.

Lucifer yellow and FM4-64 endocytosis assays

For Lucifer yellow assays, cells were grown in liquid YE5S culture with or without latrunculin A, spun down, and resuspended in YE5S (25 μl) containing Lucifer yellow dye (10 μl of 40 mg/ml; Sigma-Aldrich; made up in water and stored in the dark at 4°C) with or without latrunculin A. Cells was incubated on a tabletop rotor for 30 min at room temperature. Cells were washed two times with 100 μl of potassium phosphate buffer (50 mM potassium phosphate, pH 7.5, 10 mM NaF, 10 mM NaN_3) and imaged immediately on a Zeiss scanning confocal microscope (Zeiss, Jena, Germany). For FM4-64 assays, cells were grown in liquid YE5S culture with or without latrunculin A for 10 min, stained with 20 mM FM4-64 (Molecular Probes, Eugene, OR) for 1 min at room temperature, washed with YE5S, and imaged after 10 min.

ACKNOWLEDGMENTS

We thank members of the Chang lab, especially N. Minc, for guidance and support, Ignacio Flor-Parra and Rafael Daga for the protoplast protocol, and J. Q. Wu for strains. This work was supported by National Institutes of Health Grant R01-GM056836.

REFERENCES

Aghamohammadzadeh S, Ayscough KR (2009). Differential requirements for actin during yeast and mammalian endocytosis. Nat Cell Biol 11, 1039–1042.

Aiba H, Yamada H, Ohmiya R, Mizuno T (1995). The osmo-inducible gpd1+ gene is a target of the signaling pathway involving Wis1 MAP-kinase kinase in fission yeast. FEBS Lett 376, 199–201.

Arasada R, Pollard TD (2011). Distinct roles for F-BAR proteins Cdc15p and Bzz1p in actin polymerization at sites of endocytosis in fission yeast. Curr Biol 21, 1450–1459.

Ayscough KR (2000). Endocytosis and the development of cell polarity in yeast require a dynamic F-actin cytoskeleton. Curr Biol 10, 1587–1590.

Bahler J, Wu JQ, Longtine MS, Shah NG, McKenzie 3rd A , Steever AB, Wach A, Philippsen P, Pringle JR (1998). Heterologous modules for efficient and versatile PCR-based gene targeting in *Schizosaccharomyces pombe*. Yeast 14, 943–951.

Balaban NQ *et al.* (2001). Force and focal adhesion assembly: a close relationship studied using elastic micropatterned substrates. Nat Cell Biol 3, 466–472.

Basu R, Chang F (2011). Characterization of dip1p reveals a switch in Arp2/3-dependent actin assembly for fission yeast endocytosis. Curr Biol 21, 905–916.

Berro J, Sirotkin V, Pollard TD (2010). Mathematical modeling of endocytic actin patch kinetics in fission yeast: disassembly requires release of actin filament fragments. Mol Biol Cell 21, 2905–2915.
Boettner DR, Chi RJ, Lemmon SK (2012). Lessons from yeast for clathrin-mediated endocytosis. Nat Cell Biol 14, 2–10.
Boulant S, Kural C, Zeeh JC, Ubelmann F, Kirchhausen T (2011). Actin dynamics counteract membrane tension during clathrin-mediated endocytosis. Nat Cell Biol 13, 1124–1131.
Chang F (1999). Movement of a cytokinesis factor cdc12p to the site of cell division. Curr Biol 9, 849–852.
Chang F, Woollard A, Nurse P (1996). Isolation and characterization of fission yeast mutants defective in the assembly and placement of the contractile actin ring. J Cell Sci 131–142.
Collins A, Warrington A, Taylor KA, Svitkina T (2011). Structural organization of the actin cytoskeleton at sites of clathrin-mediated endocytosis. Curr Biol 21, 1167–1175.
Degols G, Shiozaki K, Russell P (1996). Activation and regulation of the Spc1 stress-activated protein kinase in *Schizosaccharomyces pombe*. Mol Cell Biol 16, 2870–2877.
deHart AK, Schnell JD, Allen DA, Tsai JY, Hicke L (2003). Receptor internalization in yeast requires the Tor2-Rho1 signaling pathway. Mol Biol Cell 14, 4676–4684.
Edelstein A, Amodaj N, Hoover K, Vale R, Stuurman N (2010). Computer control of microscopes using microManager. Curr Protoc Mol Biol Chapter 14 Unit 14.20.
Engqvist-Goldstein AE, Drubin DG (2003). Actin assembly and endocytosis: from yeast to mammals. Annu Rev Cell Dev Biol 19, 287–332.
Ferguson SM *et al.* (2009). Coordinated actions of actin and BAR proteins upstream of dynamin at endocytic clathrin-coated pits. Dev Cell 17, 811–822.
Flor-Parrra I, Zhurinsky J, Bernal M, Gallardo P, Daga RR (2013). A Lallzyme MMX-based rapid method for fission yeast protoplast preparation. Yeast, doi: 10.1002/yea.2994.
Galletta BJ, Cooper JA (2009). Actin and endocytosis: mechanisms and phylogeny. Curr Opin Cell Biol 21, 20–27.
Gheorghe DM, Aghamohammadzadeh S, Smaczynska-de R II, Allwood EG, Winder SJ, Ayscough KR (2008). Interactions between the yeast SM22 homologue Scp1 and actin demonstrate the importance of actin bundling in endocytosis. J Biol Chem 283, 15037–15046.
Giardini PA, Fletcher DA, Theriot JA (2003). Compression forces generated by actin comet tails on lipid vesicles. Proc Natl Acad Sci USA 100, 6493–6498.
Girao H, Geli MI, Idrissi FZ (2008). Actin in the endocytic pathway: from yeast to mammals. FEBS Lett 582, 2112–2119.
Hohmann S (2002). Osmotic stress signaling and osmoadaptation in yeasts. Microbiol Mol Biol Rev 66, 300–372.
Idrissi FZ, Blasco A, Espinal A, Geli MI (2012). Ultrastructural dynamics of proteins involved in endocytic budding. Proc Natl Acad Sci USA 109, E2587–E2594.
Idrissi FZ, Grotsch H, Fernandez-Golbano IM, Presciatto-Baschong C, Riezman H, Geli MI (2008). Distinct acto/myosin-I structures associate with endocytic profiles at the plasma membrane. J Cell Biol 180, 1219–1232.
Kaksonen M, Toret CP, Drubin DG (2005). A modular design for the clathrin- and actin-mediated endocytosis machinery. Cell 123, 305–320.
Kaksonen M, Toret CP, Drubin DG (2006). Harnessing actin dynamics for clathrin-mediated endocytosis. Nat Rev Mol Cell Biol 7, 404–414.
Kishimoto T, Sun Y, Buser C, Liu J, Michelot A, Drubin DG (2011). Determinants of endocytic membrane geometry, stability, and scission. Proc Natl Acad Sci USA 108, E979–E988.
Kovar DR, Pollard TD (2004). Insertional assembly of actin filament barbed ends in association with formins produces piconewton forces. Proc Natl Acad Sci USA 101, 14725–14730.
Kukulski W, Schorb M, Kaksonen M, Briggs JA (2012). Plasma membrane reshaping during endocytosis is revealed by time-resolved electron tomography. Cell 150, 508–520.
Liu J, Sun Y, Oster GF, Drubin DG (2010). Mechanochemical crosstalk during endocytic vesicle formation. Curr Opin Cell Biol 22, 36–43.
Merrifield CJ, Feldman ME, Wan L, Almers W (2002). Imaging actin and dynamin recruitment during invagination of single clathrin-coated pits. Nat Cell Biol 4, 691–698.
Merrifield CJ, Perrais D, Zenisek D (2005). Coupling between clathrin-coated-pit invagination, cortactin recruitment, and membrane scission observed in live cells. Cell 121, 593–606.
Merrifield CJ, Qualmann B, Kessels MM, Almers W (2004). Neural Wiskott Aldrich syndrome protein (N-WASP) and the Arp2/3 complex are recruited to sites of clathrin-mediated endocytosis in cultured fibroblasts. Eur J Cell Biol 83, 13–18.
Meyer P, Gutierrez J, Pogliano K, Dworkin J (2010). Cell wall synthesis is necessary for membrane dynamics during sporulation of *Bacillus subtilis*. Mol Microbiol 76, 956–970.
Minc N, Boudaoud A, Chang F (2009). Mechanical forces of fission yeast growth. Curr Biol 19, 1096–1101.
Mogilner A, Rubinstein B (2005). The physics of filopodial protrusion. Biophys J 89, 782–795.
Molloy JE, Burns JE, Kendrick-Jones J, Tregear RT, White DC (1995). Movement and force produced by a single myosin head. Nature 378, 209–212.
Moreno S, Klar A, Nurse P (1991). Molecular genetic analysis of fission yeast Schizosaccharomyces pombe. Methods Enzymol 194, 795–823.
Morrell JL, Morphew M, Gould KL (1999). A mutant of Arp2p causes partial disassembly of the Arp2/3 complex and loss of cortical actin function in fission yeast. Mol Biol Cell 10, 4201–4215.
Mulholland J, Preuss D, Moon A, Wong A, Drubin D, Botstein D (1994). Ultrastructure of the yeast actin cytoskeleton and its association with the plasma membrane. J Cell Biol 125, 381–391.
Nambiar R, McConnell RE, Tyska MJ (2009). Control of cell membrane tension by myosin-I. Proc Natl Acad Sci USA 106, 11972–11977.
Newpher TM, Smith RP, Lemmon V, Lemmon SK (2005). In vivo dynamics of clathrin and its adaptor-dependent recruitment to the actin-based endocytic machinery in yeast. Dev Cell 9, 87–98.
Pelham RJ Jr, Chang F (2001). Role of actin polymerization and actin cables in actin-patch movement in *Schizosaccharomyces pombe*. Nat Cell Biol 3, 235–244.
Proctor SA, Minc N, Boudaoud A, Chang F (2012). Contributions of turgor pressure, the contractile ring, and septum assembly to forces in cytokinesis in fission yeast. Curr Biol 22, 1601–1608.
Robertson AS, Smythe E, Ayscough KR (2009). Functions of actin in endocytosis. Cell Mol Life Sci 66, 2049–2065.
Schaber J *et al.* (2010). Biophysical properties of *Saccharomyces cerevisiae* and their relationship with HOG pathway activation. Eur Biophys J 39, 1547–1556.
Sirotkin V, Beltzner CC, Marchand JB, Pollard TD (2005). Interactions of WASp, myosin-I, and verprolin with Arp2/3 complex during actin patch assembly in fission yeast. J Cell Biol 170, 637–648.
Sirotkin V, Berro J, Macmillan K, Zhao L, Pollard TD (2010). Quantitative analysis of the mechanism of endocytic actin patch assembly and disassembly in fission yeast. Mol Biol Cell 21, 2894–2904.
Skau CT, Kovar DR (2010). Fimbrin and tropomyosin competition regulates endocytosis and cytokinesis kinetics in fission yeast. Curr Biol 20, 1415–1422.
Skruzny M, Brach T, Ciuffa R, Rybina S, Wachsmuth M, Kaksonen M (2012). Molecular basis for coupling the plasma membrane to the actin cytoskeleton during clathrin-mediated endocytosis. Proc Natl Acad Sci USA 109, E2533–E2542.
Taylor MJ, Perrais D, Merrifield CJ (2011). A high precision survey of the molecular dynamics of mammalian clathrin-mediated endocytosis. PLoS Biol 9, e1000604.
Veigel C, Molloy JE, Schmitz S, Kendrick-Jones J (2003). Load-dependent kinetics of force production by smooth muscle myosin measured with optical tweezers. Nat Cell Biol 5, 980–986.
Weinberg J, Drubin DG (2012). Clathrin-mediated endocytosis in budding yeast. Trends Cell Biol 22, 1–13.
Wu JQ, Bahler J, Pringle JR (2001). Roles of a fimbrin and an alpha-actinin-like protein in fission yeast cell polarization and cytokinesis. Mol Biol Cell 12, 1061–1077.
Wu JQ, Pollard TD (2005). Counting cytokinesis proteins globally and locally in fission yeast. Science 310, 310–314.